Post Flight Analysis Report

Project TELL - Spaceport America Cup 2018

Doc. Reference	TELL_FR01_Post_Flight_Analysis_01
Author	Alex Schmid (alexschm@student.ethz.ch)
Co Authors	Anna Kiener
	David Haeusermann
	Bruno Frutig
	Ziga Brencic
Date	17-May-2019

Abstract This document reports on the settings of the sounding rocket TELL and its flight at the Spaceport America Cup 2018. Being the inaugural project of the student association ARIS, TELL was designed and built to reach an apogee of 10'000 ft above ground level with a commercial off-the-shelf solid motor and recover the rocket with a dual parachute system. After 1.4s into flight, the M2400T motor caused a mission catastrophic failure due to over-pressurization from backside burning.

This report focuses on the flight events and the investigations after recovery of the remains.

Document Change History

Rev. Number	Change Description
Rev. 01	Initial Creation

Contents

1 Abbreviations

Abbr.	Description
AFT	Afterward
AT	AeroTech
AGL	Above Ground Level
Cato	Catastrophic failure
COTS	Commercial off-the-shelf
ESRA	Experimental Sounding Rocket Association
FWD	Forward
GMT	Greenwich Mean Time
HPR	High Power Rocketry
LCO	Launch Control Officer
MDF	Medium Density Fiberplate (wood)
SRAD	Student researched & developed
SA-Cup	Spaceport America Cup

2 Mission TELL and the Events

2.1 Project TELL

TELL is a sounding rocket developed by the *Akademische Raumfahrt Initiative Schweiz (ARIS)* for the *Spaceport America Cup (SA-Cup)* 2018 in New Mexico, USA. It has been launched on Thursday, 21. June 2018, at 12:29h (GMT-7). The rocket was specifically designed and built to reach a target apogee of 10'000 ft with a Commercial off-the-shelf (COTS) solid motor. All other systems of the rocket were student researched and developed (SRAD). This includes the rocket internal structure and airframe, the avionics and telemetry system, a recovery system with COTS parachutes, an Air Brake module and a payload of 5 kg on board (see Figure 1). TELL is the inaugural project of ARIS and was developed and built from scratch in less than one year from October 2017 to June 2018.

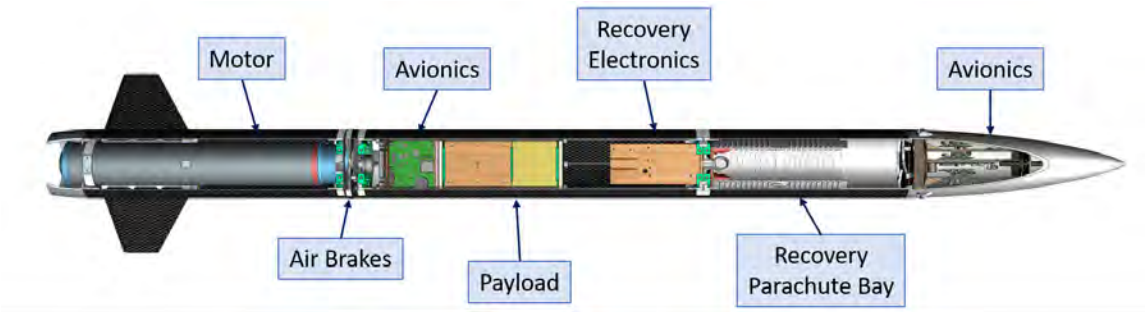

Figure 1: The CAD modell of the sounding Rocket TELL with the main subsystems.

A detailed description of the design, manufacturing and integration of the rocket TELL, its subsystems and its operational concept can be found in TELL's technical report. This report is available on the ARIS homepage *https://aris-space.ch/project-tell/* or can be requested at *contact@aris-space.ch*.

2.2 Summary of the Flight Card

The flight stability of the rocket is determined by the position of the center of mass c_m and center of pressure c_p as depicted in Figure 2. TELL's caliber, referred to as the main diameter below the nosecone, was 150 mm.

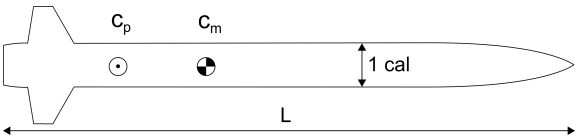

Figure 2: Characteristic aerodynamic properties of a sounding rocket.

The Table below summarizes the main performance parameters derived for the rocket TELL before its launch. The values of this Flight Card parameters indicate stable flight. The values were defined using a student written three degrees of freedom Matlab flight simulator and compared to simulations with COTS RockSim software.
For more information on the simulations contact GianAndrea Mueller or Ziga Brencic of project TELL.

Description	Value	
Motor	`Aerotech M2400 T`	
Take-off mass	`23.9424`	[kg]
Rocket length L	`2.417`	[m]
Rocket diameter	`0.1582`	[m]
Propellant Mass	`3.6926`	[kg]
Maximum center of mass c_m	`151`	[cm]
Minimum center of pressure c_p	`178`	[cm]
Launch rail exit velocity	`31.14`	$[\mathrm{m\,s^{-1}}]$
Static margin at launch rail exit	`2.63`	[*cal*]
Apogee with control	`3048`	[m]
Maximum acceleration	`117.6 (11,98 g)`	$[\mathrm{m\,s^{-2}}]$
Maximum velocity	`314.7`	$[\mathrm{m\,s^{-1}}]$
Time to apogee	`25.76`	[s]
Time to touchdown	`207.76`	[s]

Table 1: Selected values from flight card

2.3 The AeroTech M2400T Solid Motor

The rocket was propelled by an AeroTech (AT) M2400T motor. This M-class High Power Rocketry (HPR) motor has a total impulse of 7716.5 Ns during 3.2 s of burn time. It contains three grains of Blue Thunder propellant, a fast burning propellant and is delivering an average thrust of 2400 N while reaching thrusts up to 2700 N according to specifications (e.g. *www.thrustcurve.org*).
Figure 3 represents the assembly of the motor. In the most recent versions, grains are separated by additional O-rings to control the burning surface between the individual grains.

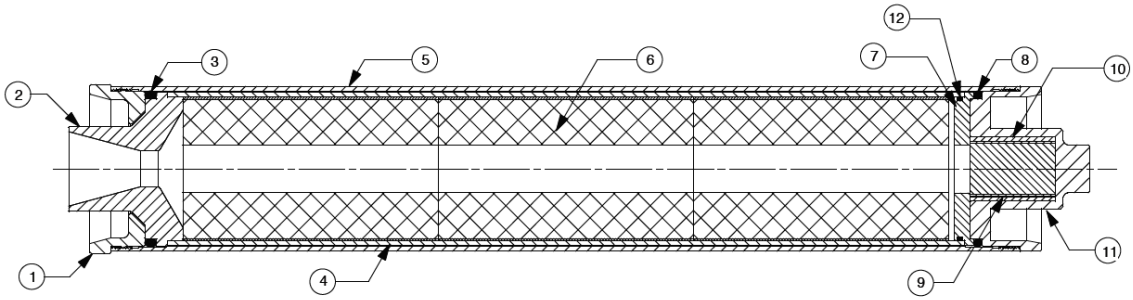

Figure 3: Drawing of the AT M2400T assembly. 1) AFT Closure 2) Nozzle 3) AFT O-ring 4) Casing 5) Phenolic Liner 6) Propellant Grain 7) Seal Disk 8) FWD Closure O-ring 9) Smoke Charge 10) Smoke Charge Insulator 11) FWD Closure 12) Seal Disk O-ring.

The motor is composed of reusable hardware (casing, closures, seal disk) as well as a reload kit for one-time usage. The casing and AFT closure of TELL were used in a previous flight, the FWD closure had never been used before. The assembly of the motor is completed by a flight operator and must follow the instructions delivered by the manufacturer to guarantee functionality. All commercial products experience quality control processes and are considered as very reliable but prone to a small statistical probability of failure.
For more information on the motor contact Alexander Schmid of Project TELL.

2.4 Description of Events

The flight experienced nominal pre-flight procedures with all checklists completed. The rocket was transported and loaded to the launch rail provided by Doug Gerrard from Rocketry Photography. All preparations went flawless and the pad could be cleared successfully. Although being first of the launch salvo, the time on the launchpad exceeded one hour, due to radio interference of ESRA's different radio systems. After a successful ignition, the rocket lifted off and cleared the launchpad nominally. Tilt and/or rotation of the rocket could be observed after leaving the launchpad. Later during the boost phase, the lower body of the rocket violently disintegrated without any previous indication. Multiple debris could be observed on trajectories pointing away from flight direction, some of them glowing, while the main body continued its flight. The main chute was spotted descending freely immediately after CATO, indicating premature separation of the nose cone. Overall, the flight until CATO lasted 1.4 s.

Time (local)	Event
11:20	Rocket installed on launch rail
12:29	Ignition
12:29	Rocket cleared launchpad
12:29	Cato/Loss of connection

Table 2: Timeline of launch events

After CATO, all launch operation were seized until emergency services responded that no fire at the launch site was observed. The salvo was continued until all rockets were launched. The ground recovery team of ARIS departed to recover all parts of the rockets, previously spotted and collected by Range Managers and other rocket teams in a radius of approx. 100 m from the launchpad. All

parts were collected for mandatory post flight inspection by ESRA. With this inspection, the flight was officially regarded complete.

3 Post CATO Evaluation

After the CATO, all components of TELL were analyzed and evaluated in order to identify potential failure sources. The following sections summarize the results from visual inspections (see Section 3.1), analysis of the Flight Data (see Section 3.2) and inputs from external experts (see Section 3.3).

3.1 Visual Inspections

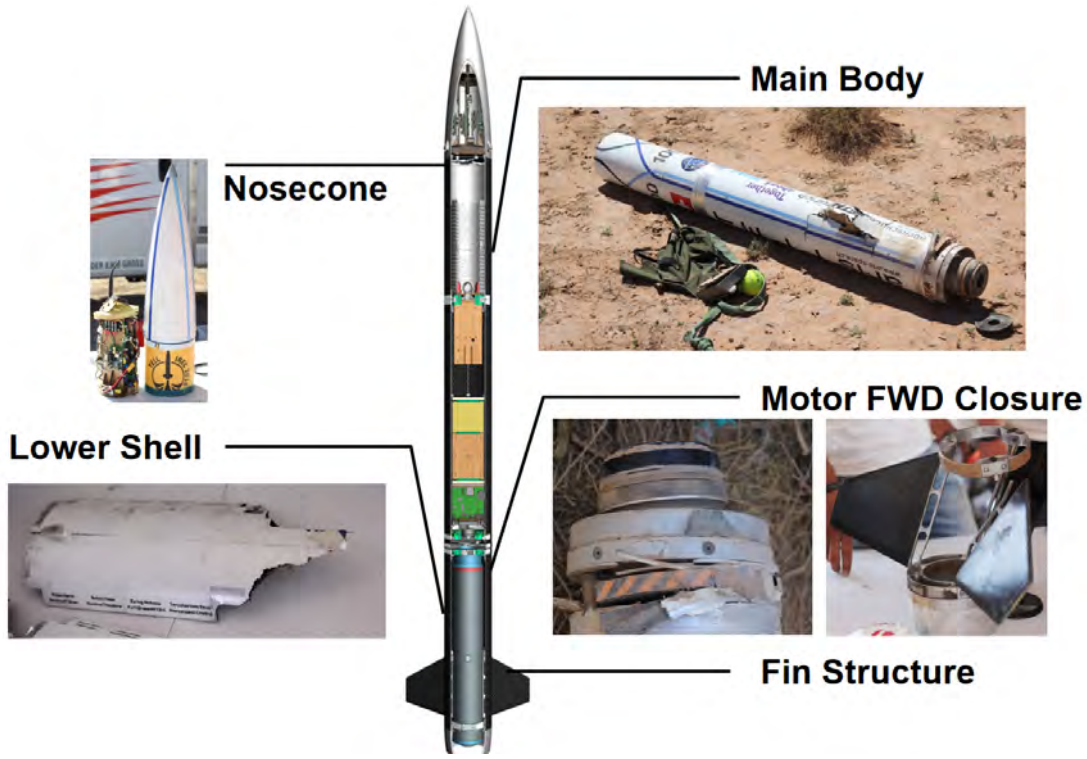

Figure 4: Overview of the found remainings of TELL

3.1.1 Visual Inspection of the Nosecone

The nosecone glassfiber structure only showed minor signs of damage. The only obvious damage is the vertical cut along the coupler section (see Figure 5). The bulkring disintegrated from the nosecone structure (see Figure 6). However, the drogue parachute was still attached to the nosecone bulkhead. For more information on the nosecone contact David Haeusermann of Project TELL.

Figure 5: The glassfiber structure is mainly intact, vertical rupture at coupler section. Bulkring separated from glass fiber structure. Avionics module was removed from the nosecone for disarming process

Figure 6: The bond of the bulkring to the glass fiber structure failed. Drogue parachute still attached to the nosecone bulkhead. The Figure shows state at recovery

3.1.2 Visual Inspection of the Middle Body, Inner Structure and Air Brakes

The Middle Section was the most damaged part of the rocket (see Figure 7). The compact ballast mass of 4.25 kg, located in the center of the Middle Body, crashed through the whole Middle Body due to the landing shock. On its way, it compromised the complete inner structure. It did not only damage the payload and lower body avionics, which were located right below it, but also the carbon fibre shell of the rocket itself (see Figure 8).
The air brakes were mostly damaged due to the over-pressurization and explosion of the COTS motor, as they were located right above the fixation of the motor.
For more information on the Structure contact Andrea Nessi or David Haeusermann, concerning the air brakes contact Serjosha Robmann.

Figure 7: The Middle Section of the Rocket TELL at ground recovery

Figure 8: The Hole caused in the airframe by the ballast mass

3.1.3 Visual Inspection of the Lower Body

The lower airframe disintegrated due to the explosion of the motor located inside. The motor adapter as well as the front closure were still attached to the motor bulkhead (see Figure 9). However, the bond joint of the carbon fiber tube and the field joint was destroyed. The field joint itself was still firmly bolted to the motor bulkhead.
The carbon fiber tube was ruptured and recovered in four pieces. The sections in between the fins were torn from the remaining tube. The rupture occurred from the edges of the cutouts for the clamps at an approximate angle of 45 degrees (see Figure 10). Furthermore the remaining tube shows a rupture along half of the circumference.
The fin can structure showed major distortions along its vertical axis (see Figure 11). One backbone was ruptured close to its attachment points. However, the sandwich panel construction of the fins showed no obvious signs of damage or distortions. This also applies for the AFT ring, the clamps and the boattail, whereas the FWD ring is slightly deformed.
For more information on the lower body contact David Haeusermann.

Figure 9: The lower body after touch down: The Motor adapter and motor front closure are still joined and also attached to motor bulkhead, while the field joint separated from the carbon fiber tube

Figure 10: The lower airframe with the liner insulation of the motor (top right) and two carbon fiber partitions and the recovery location

Figure 11: Distorted fin with partially ruptured backbone, slightly bent upper fin ring and the almost undamaged lower fin ring and boattail

3.1.4 Visual Inspection of the Motor

Although a motor failure includes a considerable amount of energy and gas liberated in short time, most parts of the motor were recovered.
The FWD closure was still attached to its adapter, but separated from the lower part of the motor. The motor casing, AFT closure an nozzle remained assembled and no serious damage is observed on the lower part and on the casing itself. The liner was found outside the casing, chipped on one site, all casting tubes and grains were pushed out. No all grains burned through completely. No adhesive residues were observed in the inside of the liner. The FWD closure and Seal Disk O-rings were located above the motor adapter. All metal parts were intact. After cleaning, the first approximately three threads of the FWD closure exhibited completely worn down teeth. For more information on the motor, contact Alexander Schmid.

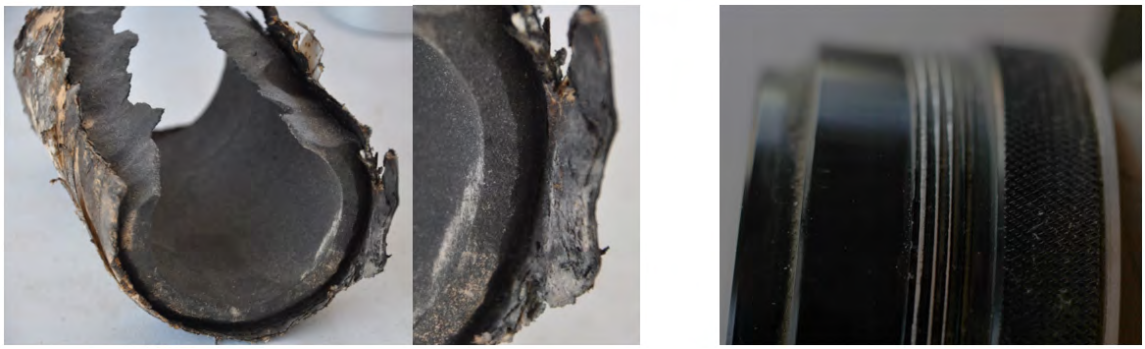

Figure 12: State of the grain (two left pictures) and the thread

3.1.5 Visual Inspection of the Recovery System

After the explosion, it was observed that the recovery system was ejected prematurely. At some point, the Kevlar cord was disrupted (see Figure 13). The drogue parachute was still attached to the nosecone after ground recovery - it is assumed that it slowed down the descent of the nosecone (see Section 3.1.1). The rest of the rocket landed without any deceleration of a parachute. Not only the cord but also the parachutes and the parachute bag were recovered in a disrupted state (see Figure 14).

Figure 13: The Kevlar chord after ground recovery

Figure 14: The torn Drogue parachute after ground recovery

3.1.6 Visual Inspection of the Nosecone Avionics

The whole avionics was built on custom made Printed Circuit Boards (PCB). Most components were soldered on the PCBs with a vapor-phase oven and all the others by hand with a soldering iron or hot-air. All cable connections had either a screwing lock or were secured with silicon (pin headers only). The connectors of the cables were all crimped except the power cables which were heavily soldered.

The shock of the explosion or of the touch down destroyed the MDF plate connecting the avionics and the nosecone bulkhead (see Figure 15). As a result of this the avionics were pushed into the nosecone. The 900 MHz antenna and the remaining upper MDF plate absorbed most of the remaining shock, leaving most of the nosecone avionics completely unharmed. Although the GPS antenna and the 2.4 GHz antenna were ripped off and the cables broke, the actual connectors on the side of the main avionics were completely intact. Also the camera cable was completely ripped off (potentially due to the sensitive nature of the PI-Cam, something that also happened during assembly). The nosecone avionics was still beeping at recovery and was still recording data.

Figure 15: The separated nosecone bulkhead which was attached to the lower MDF plate of the nosecone avionics

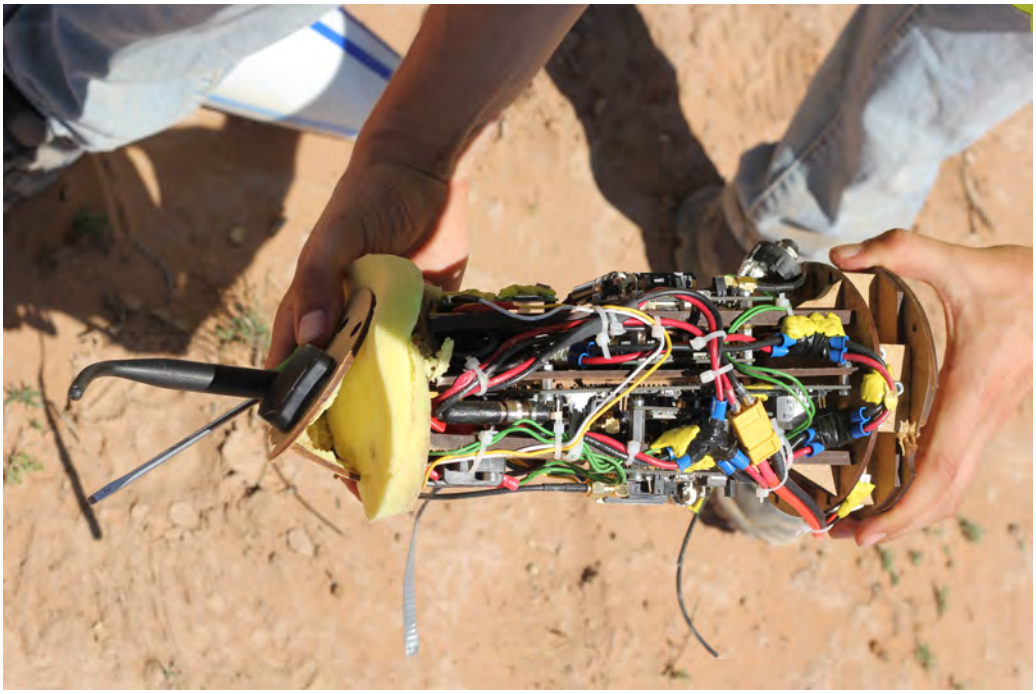

Figure 16: The recovered nosecone avionics with the bent 900 MHz and GPS antenna, and the intact cable ties in the middle connections

3.1.7 Visual Inspection of the Lower Body Avionics

The lower body avionics were completely destroyed. Almost all components were ripped off the lower body PCB plate, potentially due to the tungsten ballast plates. The Xbee PCB in the recovery was in a good state. However, the power connector and the header pins were bent and the cable for the antenna was ripped off. The heavy and beefy antenna and DB9 connectors were completely intact. The cables itself were mostly either broken in the middle or at the crimping point. For more information on the avionics software contact Raphael Schnider, for the hardware contact Alessandro Forino.

Figure 17: Completely destroyed lower body avionics and the PCB with all components ripped off

Figure 18: The lower body avionics PCB after the crash

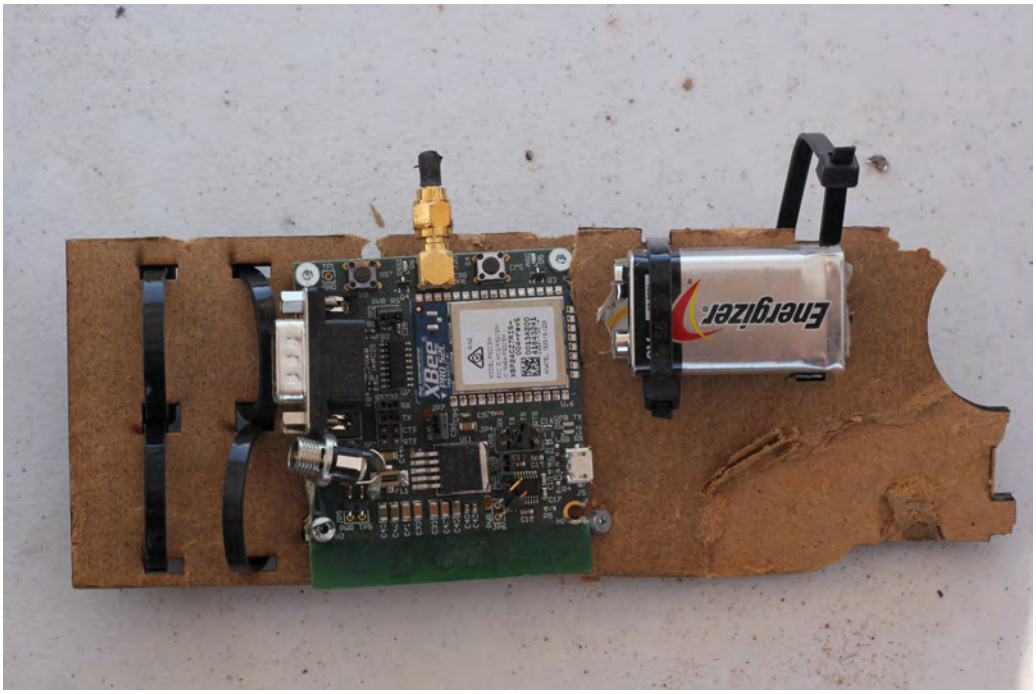

Figure 19: The Xbee module in the recovery bay with bent header pins and power connector; the components are still in place and the other connectors survived

3.1.8 Visual Inspection of the Payload

The payload section was severely damaged by the 3 kg tungsten ballast mass located directly above the experiment. This ballast was actually mounted as part of the overall payload and was torn out of its support during the impact. It struck the experiment and made the payload useless for further experiment evaluation.
Figure 21 shows the damage of the experiment from top-view and side-view. The microscope was torn from its holder due to the impact of the dummy payload (Fig: 21b). Due to the resulting high acceleration, the microscope was completely destroyed. No video data could be restored.
For more information on the payload contact Bruno Fruttig.

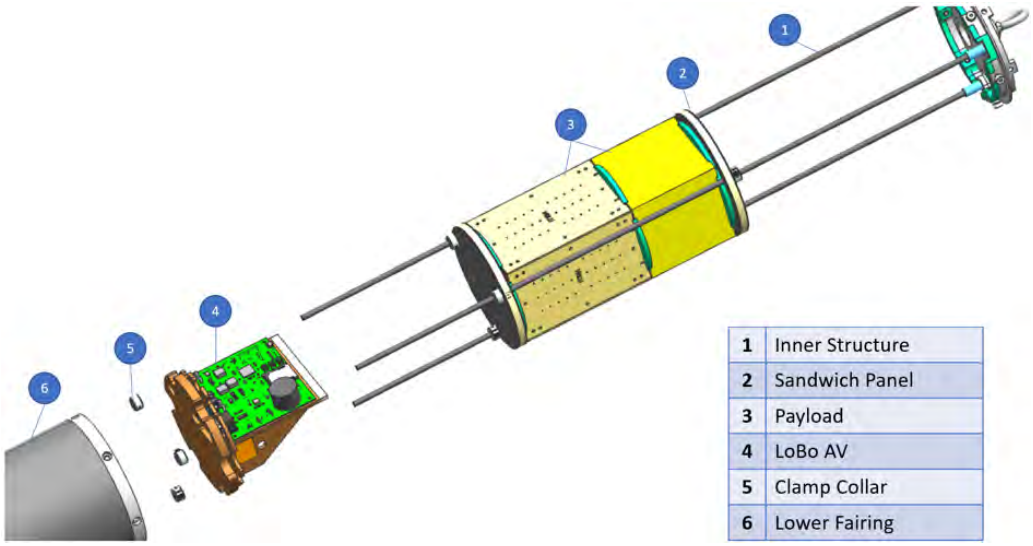

Figure 20: CAD model of the inner structure and the position of the payload

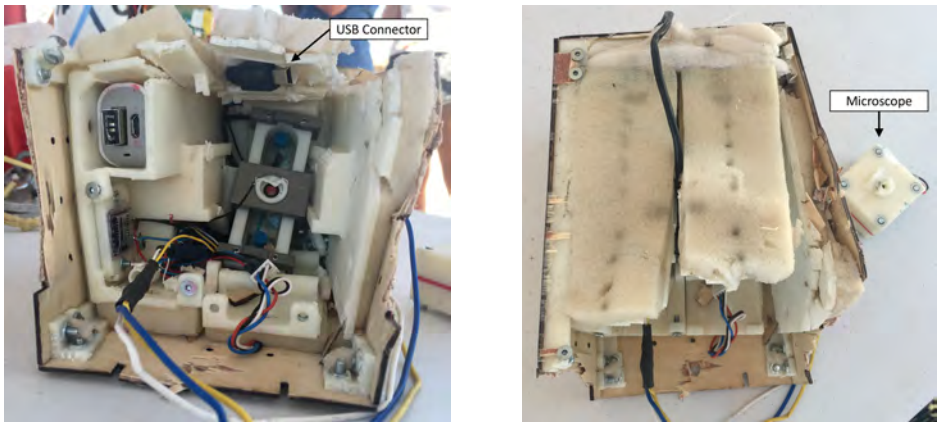

(a) Damage Experiment Top-View (b) Damaged Experiment Side-View

Figure 21: Damaged Experiment

3.2 Flight Data

3.2.1 Thrustcurve

Besides visual inspection, the thrust curve obtained from flight data is the most important feature to conclude on the motor's performance. Table 3 shows an overview of the data collecting systems inside TELL and which data they were intended to collect:

Subsystems		**Sensor**	**Data**
Recovery	Altimeter 1: Marsa 54 LHD	Accelerometer Barometer	Acceleration Pressure
	Altimeter 2: Altimax G3	Accelerometer (±105 g) Barometer	Acceleration Pressure
Avionics	SRAD Nose Cone avionics	Accelerometer Gyroscope Climate Sensor Magnetometer	Acceleration Pressure Temp., Humidity, Pressure Compass
	SRAD Lower Body avionics	Accelerometer Gyroscope Climate Sensor Magnetometer 2x Barometer	Acceleration Pressure Temp., Humidity, Pressure Compass Pressure
Payload	Arduino	2 Accelerometers	Acceleration

Table 3: Data acquiring systems

From the measured acceleration, the thrust of the rocket can be calculated. During the flight, the three major forces acting on a rocket are thrust T, gravity and drag.

$$F_{tot} = F_g + F_d + T = m_t \cdot g + \tfrac{1}{2}\,\rho\, v^2\, C_D\, A + m_t \cdot a_T = m_t \cdot a_{eff} \tag{1}$$

Here, m_t is the mass of the rocket at time t, $g = -9.8\frac{m}{s^2}$, v the velocity, C_D the coefficient of drag and ρ the density of air. At low velocities, the drag is neglected (error increases effective T). Therefore, the relation

$$m_t \cdot g + T = m_t \cdot a_{eff} \tag{2}$$

remains. Following, the thrust is determined as

$$T = m_t\ (a_{eff} - g)\,. \tag{3}$$

Note that most accelerometer's raw data express proper acceleration, not coordinate acceleration. The influence of gravity is only measured when the rocket is on the launchpad before lift off. Once in flight, no correction is required. However, when the data is processed by software, the correction for gravity is made to obtain coordinate acceleration to integrate the acceleration and obtain velocity and location of the rocket. In this case, the gravity correction must be subtracted

Figure 22 shows the ideal thrust curve acc. to the manufacturer compared to the recalculated thrust curve from multiple datasets measured during the launch of TELL.

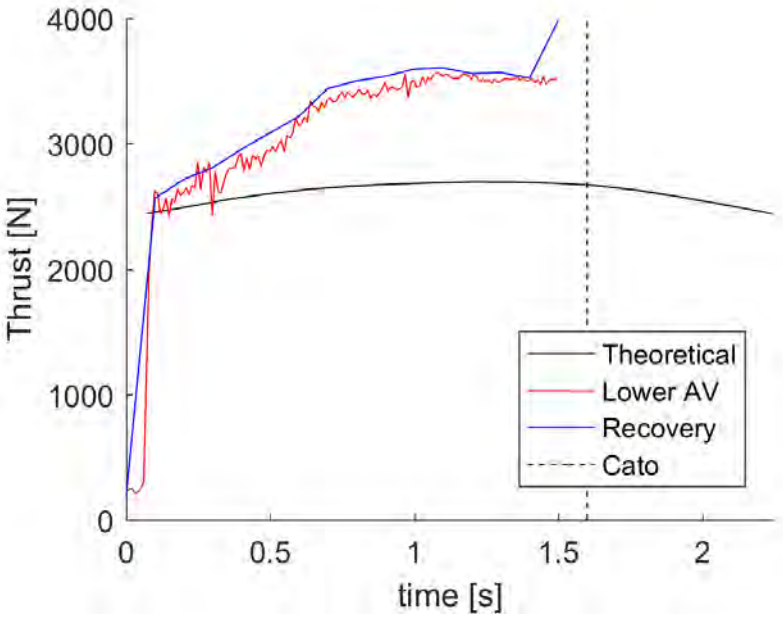

Figure 22: Recalculated and nominal thrust versus time during launch and shortly before cato.

Starting at nominal thrust, the motor shows progressive burn to high thrust values. With a peak thrust of nearly 3600 N, the motor exceeded its nominal max. T by one third. The individual sensor datasets correlate to a large degree, cross validating the infromation obtained. This is important for two reasons, one being the SRAD character of the rocket's avionics and the other the possibility for damaged, corrupted data as a consequence of the non-nominal flight event. The recalculated thrust curves show that the motor performed out of its nominal range. Such an observation can be made if the propellant's burning rate is higher than planned or the nozzle throat is not properly dimensioned. In both cases, the next level cause is higher chamber pressure, forcing the gas to be expelled at larger velocities and causing larger thrust values.
For more information on the thrust curve contact Alex Schmid.

3.3 Inspections by External Experts

Traditionally, motor catos gather a lot of attention from all parties involved. Therefore, ARIS was able to get valuable opinions of HPR experts, which shall be summarized in this paragraph.

Randy Marek, Flight Safety Reviewer, Judge, ESRA:
Mr. Marek officially inspected the recovered parts of the rocket and agreed to have an additional view on the casing. After cleaning the threads of the casing and closure, he stated:

- The casing clearly shows the signs of a overpressurization. The thread of the FWD closure is worn down on the first three turnings, the load bearing part of any thread.

Robert DeHate, Owner of Animal Motorworks (AMW), primary onsite vendor:
Mr. DeHate analysed the recovered grain the day after the launch in detail. According to his opinion, the grain failed due to backside burning. He noted:

- Normally, grains extinguish immediately at motor cato due to the sudden pressure drop to atmospheric pressure from burning chamber pressure. The fact that grains continued to burn for a while suggests that the pressure drop was slowed down by pressurization of the lower rocket body.
- Based on the measurements from the remaining propellant, the grain recovered burned 50-60% of its propellant before cato.
- The grain recovered shows anomalies on the backside between the casting tube and the propellant.

Backside burning: When propellant of a grain does not bond nominally to its casting tube, the flame can penetrate in between. This increases the burning area and causes the pressure to increase. A common outcome of this behaviour is an overpressurization of the motor, leading to a cato.

Joe Hinton, Owner of MotoJoe, supplier of ARIS:
Mr. Hinton informed ARIS in an e-mail that a day after the cato of TELL during its boost, another team, the Texas - Rio Grande team, experienced a cato. The rocket was propelled by aa AT M2500T, a motor using the same type of propellant as the AT M2400T used in TELL.

Charles Savoie, General Manager of RCS RMC Inc.(AeroTech), manufacturer of the motor:
Mr. Savoie immediately inspected the hardware recovered by Doug Gerrard after he was notified by Mr. Gerrard. Without the recovered grain and puzzled by the final position of the O-rings, he initially suggested an assembly error as the most possible cause of failure. After presenting the collected grain and evidence to Mr. Savoie, he forwarded the case to Mr. Karl Bauman.

Karl Baumann, Vice President, R&D and Facilities, RCS RMC Inc.(AeroTech):
'From the photographic evidence and incidental observations made by you and your team , the root cause of the motor failure was: Propellant grain edge burning, the result being the over pressurization of the motor case, causing it to fail forward along its longitudinal axis.'

Edge Burning: 'The [...] phenomena can be induced by a higher than nominal burn rate, which increases internal motor pressure which exploits the propellant to casting tube bond, exposing the propellants surface to the flame front, rapid over pressure results.'

4 Discussion and Conclusions

4.1 Structures: Nosecone

It is assumed that the apogee detection system triggered the CO2 system to eject the nose cone and the drogue chute right after the explosion of the motor. This caused the nose cone to separate from the rest of the airframe. The airframe however was still ascending along its initial trajectory.

This leads to the nose cone not being propelled anymore and being tilted sidewards. The kevlar cord cutting is then tensioned and cuts through the coupler section of the nose cone while the nose cone continues tilting.

The nose cone eventually starts pointing downwards. Its drag and inertia still tensions the kevlar cord which is attached to the main parachute release system. The chord cuts through the carbon fiber tube and is severely damaged in the process which leads to a rupture of the cord.

4.2 Structures: Middle Body and Inner Structure

As conclusion it must be stated that a payload functioning only as dummy mass with a weight of several kilos is critical, as well as its placement above sensitive systems as the scientific payload or the lower body avionics.

It is suggested to have more strict mass requirements for the scientific payload. Furthermore, several locations within the rocket shall be designed to add or remove spare weight easily. Also, no low cost MDF shall be used for structural parts (as it was used for the lower body avionics and also the structure of the dummy mass).

4.3 Structures: Lower Body

The cause for the rupture of the lower airframe tube is the pressurization of the airframe after the explosion of the motor. After the explosion burning propellant was observed. Usually the propellant is extinguished due to the sudden pressure drop in case of a closure failiure. During the investigation of the debris and the discussion of the observations it was mentioned by a judge that the occurrence of burning propellant after the explosion underlines the sturdy construction of the lower airframe as it could withstand a certain level of pressure before rupturing.

It is assumed that the pressurization caused the carbon fiber sections in between the fins to rupture simultaneously, releasing the fin can from the lower airframe. The rupture was initiated at the sharp corners of the cutouts for the clamps. The rupture propagated through the composite material at 45 degrees. Due to the impulse induced by the sudden opening of the forward closure the motor casing was propelled in the opposite of the launch direction. Due to the high acceleration of the motor casing the friction fit between the casing and the aft fin can ring could not keep the motor retained inside the fin can.

Therefore the disintegrated carbon fiber tube, the motor casing as well as the fin can descended individually. Eventually the circumferential rupture of the tube was caused by the impact on the ground. The same is assumed for the distortion of the fin can. Most probably it tumbled during the descent and touched ground first with the forward aluminium ring. This impact causing the deformation of the forward ring and the distortion of the backbone structure due to the sudden deceleration of the heavy boattail and the resulting compression force acting on the rest of the fin can structure.

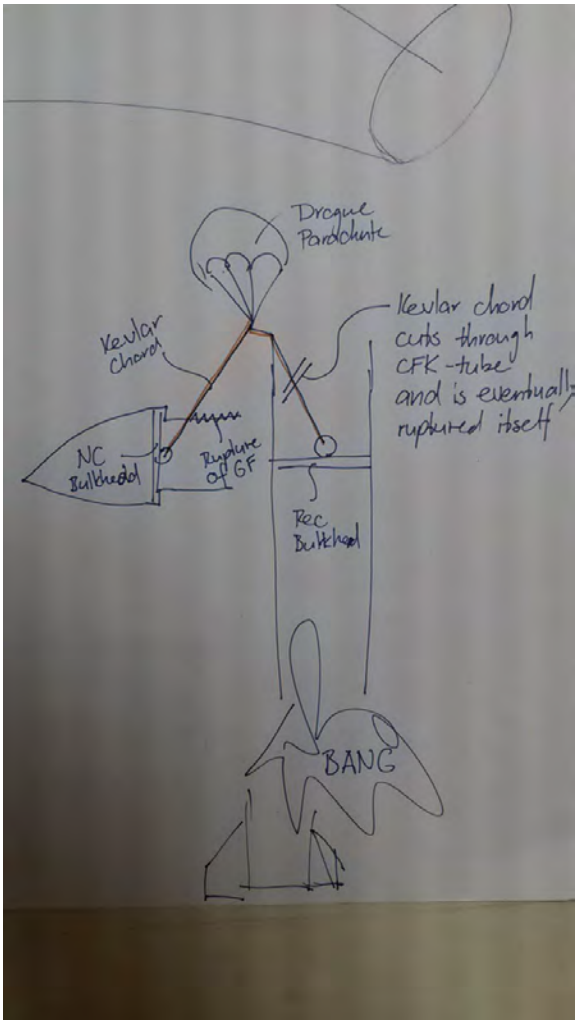

Figure 23: Sketch of a possible explanation of events which led to the separation of the nose cone and the drogue parachute from the main airframe

The minor damage of the nose cone is most probably due to the fact that the drogue parachute was still attached to the nose cone which slowed the descent rate. Most probably the bulkring was still attached to the glass fiber structure during the descent of the nose cone. It was bonded behind the recess for a smooth transition from the nose cone to the parachute tube above the coupler section. Therefore the attachment of the bulkring was a form fit which hindered the rupture of the bulkring out of the glass fiber structure opposite the direction of intended launch. Obviously the bond did not secure it sufficiently in the opposite direction which led to a rupture of the bond line during ground impact.

4.4 Motor

In conclusion to the recovered parts and discussions with experts, it can be stated that the COTS motor failed. Due to propellant grain edge burning, an over pressurization occured causing the flight of TELL to fail.

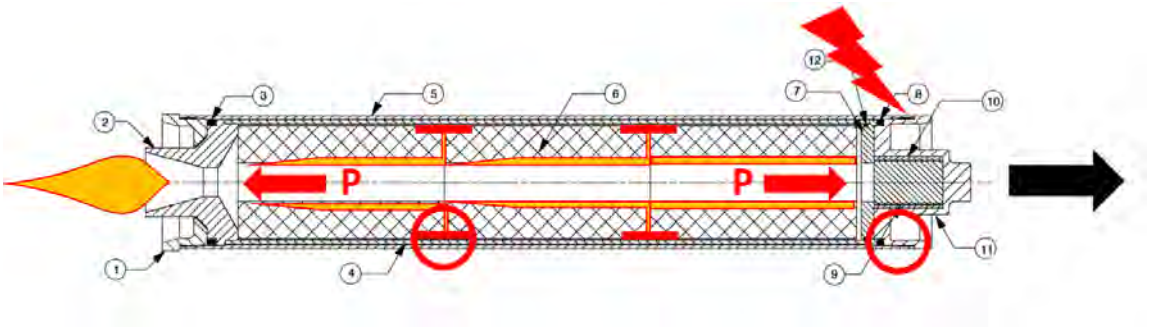

Figure 24: Depiction of irregular grain burning, leading to over pressurization and the failure where the motor was attached to the structure

4.5 Recovery

Due to the motor explosion the COTS flight computer must have triggered the ejection of the recovery system falsely. The ejection was designed to be triggered at apogee where the speed of the rocket should already be decreased. At the point of the explosion, the speed was much higher than it would be at apogee, causing a much higher shock force due to the parachute ejection. This explains the rupture of the parachutes and the kevlar chord.

4.6 Avionics: Nosecone and Lower Body

As a conclusion we can make the following statements:

- Crimping forms a strong connection, but represents still the weak spot in the connection.
- Soldering was completely reliable and formed very strong connections, however this is due to the fact that only the very big cables of the power connectors (AWG 16) were soldered and this was done very cautious.
- Cable ties were the most reliable solution forming extremely strong friction points which were much stronger than the cables we used.
- Soldering with a vapor phase oven as well as by hand was reliable enough and caused no problems whatsoever during the launch and the explosion.
- All components and connectors that can bend should be avoided (e.g. header pins, power connectors used).
- Through-hole connectors which cannot bend proved to be strong enough and did not represent a weak point.

4.7 Payload

Although the payload was severely damaged, the acceleration values could be restored. These rise rapidly after launch to almost 17g and then abruptly abort. In Figure 21a it can be seen, that the USB connector on the Arduino is no longer plugged in, even though it has been aligned so that the acceleration of the rocket pushes it into its socket. That the free fall of the rocket can not be recognized in the data can be explained by the fact that the USB plug was pulled out of its socket by the abrupt deceleration of the experiment after rocket failure which corresponds to a high

acceleration contrary to the expected direction.

Whether the Arduino and the accelerometers have also been damaged or whether they still work can only be said after another detailed look at the experiment is made.

5 Project Conclusion

Although the flight of project TELL was no success, the students learned and grew through its outcome. Initially, wrong handling of the motor or a failure of the rocket structure were thought to be the origin of the cato. A proper and thorough flight analysis was conducted with experts, helping to find the real cause of the cato and gather a better understanding of the complexity of a rocket system. This analysis sets a base for the second sounding rocket project of ARIS. The outcome also emphasizes how important tests, be it subsystem tests or full flight tests, are for a successful mission.